R. & M. No. 3317

MINISTRY OF AVIATION

AERONAUTICAL RESEARCH COUNCIL
REPORTS AND MEMORANDA

Measurements of Free-Stream Turbulence in some Low-Speed Tunnels at N.P.L.

By P. BRADSHAW, B.A. and D. H. FERRISS, B.Sc.
OF THE AERODYNAMICS DIVISION, N.P.L.

LONDON: HER MAJESTY'S STATIONERY OFFICE
1963
NINE SHILLINGS NET

Measurements of Free-Stream Turbulence in some Low-Speed Tunnels at N.P.L.

By P. Bradshaw, B.A. and D. H. Ferriss, B.Sc.
of the Aerodynamics Division, N.P.L.

*Reports and Memoranda No. 3317**
January, 1962

Summary.

The r.m.s. fluctuation levels in the older low-speed tunnels at N.P.L. are found to be as follows: Compressed Air Tunnel, 0·3% rising to 0·6% at maximum speed and pressure; 13 ft × 9 ft Tunnel, 0·05 → 0·2%; 9 ft × 7 ft (South) Tunnel, 0·18%; 18 in. Anemometer Tunnel, 0·2% in the unrestricted tunnel rising to 1% when running with diaphragms at low speed.

Introduction.

Detailed measurements of the turbulence in the N.P.L. low-speed tunnels have not previously been made, and when information about the turbulence in the Compressed Air Tunnel was needed, the opportunity was taken to investigate some of the other tunnels as well. The results are presented here with a description of the tunnels and a short discussion of the likely sources of turbulence in each. Although intended chiefly for the information of those who use the tunnels it is hoped that the results will also be useful to tunnel designers.

The authors wish to acknowledge the help of Mr. M. T. Gee, formerly of the Aerodynamics Division, N.P.L., in the planning and direction of the experiments. Messrs. R. J. Easton and K. W. Stuart assisted with the experimental work.

Apparatus.

The measurements in the 9 ft × 7 ft, 13 ft × 9 ft and 18 in. Anemometer Tunnels, and some earlier measurements in the C.A.T., were made with constant-current hot-wire apparatus, purchased from Dr. G. Dätwyler of Zürich. The amplifier has resistance-inductance frequency compensation and a bandwidth of about 30 kc/s. With the wire sensitivities and time constants of the present experiment, the noise level corresponded to about 0·07% turbulence. The wires were 0·0002 in. diameter platinum. 0·0003 in. platinum and 0·00015 in. platinum-rhodium were also used in an unsuccessful attempt to avoid wire breakage due to vibration at high pressures in the C.A.T. Single-wire probes were calibrated in the tunnel where they were used, but the cross-wire probes were calibrated in mean speed and in yaw in a 1 in. square pipe in turbulent flow.

The second set of measurements in the C.A.T., reported here, was made with DISA 55A01 constant-temperature anemometers. The noise level is quoted by the makers as equivalent to 0·06% r.m.s. turbulence with a 6 kc/s bandwidth, and was measured as 2mV with approximately this bandwidth. It probably increases proportional to the square root of the bandwidth, but should

* Replaces N.P.L. Aero Report No. 1001—A.R.C. 23,483. Published with the permission of the Director, National Physical Laboratory.

in any case be small compared with the turbulence in the C.A.T.: a good signal-to-noise ratio was maintained up to about 15 kc/s as can be seen from the spectra. 0·0002 in. diameter tungsten wires were used. The single-wire probes were calibrated in the tunnel, and the cross-wire probes were calibrated in mean speed and yaw in the core of a 2 in. diameter jet.

In the 13 ft × 9 ft and Anemometer Tunnels, spectra were measured on a Muirhead D788A analyser with a frequency range of 3 c/s to 3 kc/s. This analyser is of the Wien bridge constant-percentage-bandwidth type with a Q of 10, and its reliability at the low-frequency end of a wide-bandwidth spectrum is exceedingly doubtful as the off-tune rejection never exceeds about 40 dB. However, a high-Q analyser is preferable if discrete frequencies are expected. In order to show up discrete frequencies, the analyser r.m.s. output, proportional to $\sqrt{\{f\overline{[u(f)]^2}\}}$ has been plotted against $\log f$. Spectra in the C.A.T. and 9 ft × 7 ft Tunnel were measured with a Bruel and Kjaer 2111 $\frac{1}{3}$-octave analyser with a frequency range of 16 c/s to 31·5 kc/s: it had been found previously that there were no sharp peaks in the spectrum and as accurate readings at low frequency were desired the passive-filter analyser was preferable to the Muirhead type. These spectra are recorded here in the usual form for turbulence spectra, $F = \overline{[u(f)]^2}/\overline{u^2}$, instead of $\sqrt{\{f\overline{[u(f)]^2}\}} \propto \sqrt{(fF)}$, being plotted against $\log f$.

More details of the apparatus and measurement techniques are given in Ref. 1.

In the Anemometer Tunnel tests the probes were mounted on a rod secured outside the tunnel structure: in all the other tests the probes were mounted on a heavy steel bar, freely suspended within a hollow steel strut screwed to the tunnel structure, as shown in Fig. 5.

Description of Tunnels and Results.

1. *The Compressed Air Tunnel* (*Fig.* 1).

This tunnel was built in 1930. It has a 6 ft diameter open-jet working section and an annular return circuit, the whole being enclosed in a pressure shell. The maximum working pressure is 25 atmospheres absolute and the maximum speed 90 ft/sec, giving a Reynolds number of $1{\cdot}4 \times 10^7$ per foot. A 2-bladed fan is driven by a 400 h.p., 800 r.p.m. electric motor. The tunnel is largely used for tests of models of prototype aircraft. Since its construction improvements to the flow have been made by fitting vanes to prevent separation at the annular 180° bend ahead of the contraction, and by fitting a 2 in. deep precision honeycomb with right-angled triangular cells having an apex to hypotenuse spacing of $\frac{1}{4}$ in., but the mean velocity variations and turbulence intensity are worse than in more modern tunnels, owing to the relatively sharp bends and the small contraction ratio. As far as it is possible to judge, these flow conditions have not caused serious discrepancies between C.A.T. model tests and full-scale results.

Two sets of measurements of the tunnel turbulence have been made. The first tests were conducted in May, 1960 with constant-current hot-wire apparatus: trouble was experienced with probe vibration and wire breakage at the higher pressures, and the compensation time constant on the hot-wire apparatus could not be reduced below 0·2 milliseconds. The results of these tests are not presented. The second tests were conducted in May, 1961 with constant-temperature apparatus, stronger probes and tungsten wire. The probes again tended to vibrate at high dynamic pressures, and results obtained with severe vibration have been omitted from the graphs. Large-amplitude vibrations of the probe could be seen on the closed-circuit television screen when they occurred. The results have been plotted against Reynolds number per foot at the different pressures but there is no particular reason why they should all collapse together on this scale: the scatter in

the results under similar conditions of Reynolds number per foot, U/ν, *and* working pressure is probably due to contamination of the wires by dust, as there has never been any indication of non-repeatability in force measurements on models. Differences in the turbulence measurements at the same value of U/ν but at different working pressures are in part due to the vibration of the probe relative to the heavy main-tunnel structure, and in part to the effect of vibration of some lighter parts of the tunnel structure.

The longitudinal component of turbulence lies between 0·3 and 0·4% at the lower speeds and pressures but rises to 0·6% at the maximum speed at pressures of about 200 p.s.i. and above (Fig. 6). A value of 0·8% was recorded on one occasion at 350 p.s.i. and high speed, when the probe and its support bar were vibrating noticeably: this was the worst fit of vibration noticed, but there is undoubtedly some contribution from probe vibration in the results at the higher pressures. As there was no trace of discrete frequencies in the spectra (Fig. 8) it may be assumed that the probe was responding to random excitation as a solid body rather than suffering from prong resonance as was found with the weaker probes in the first tests. The probe stand was attached to a lighter part of the tunnel structure than that normally used for mounting models: it is unlikely that buffeting of the stand contributed any greater proportion of the apparent turbulence reading in the C.A.T. than in the other tunnels for which this stand was used.

The tests were made with a large swept-wing model in the working section, well behind the probe. As seen in Fig. 6b, no very significant increase in turbulence resulted from an increase in model incidence from zero to 22°.

The lateral component was also measured, on an axis parallel to the axis of the probe stand so that any vibration of the probe arm with respect to the stand should have had little effect. Again, the recorded turbulence increases with increasing pressure for any given fan speed (Fig. 7), and again the spectrum is largely composed of low-frequency contributions (Fig. 9). It is felt that these low-frequency components of turbulence and vibration might cause discrepancies between flight tests and C.A.T. model tests in respect of maximum lift. A 0·5% vertical-component r.m.s. intensity implies an r.m.s. incidence fluctuation of $\frac{1}{4}°$, and deviations of incidence up to $\pm \frac{3}{4}°$ will be not uncommon, so that an aerofoil set at a mean incidence just below that for maximum lift will stall prematurely: the average lift obtained will therefore be too low. At high working pressures but low wind speeds the v-component r.m.s. intensity rose to 0·5 or 0·6%, but the observations have been omitted from Fig. 7 because in practice the corresponding Reynolds numbers would be obtained by running the tunnel at a higher speed and a lower pressure. The u-component, however, did not rise to a similar extent.

The conclusion from the C.A.T. tests is therefore that the apparent turbulence rises considerably at the higher speeds and pressures chiefly because of vibration.

2. 13 *ft* × 9 *ft Tunnel*[2] (*Fig.* 2).

This is the largest tunnel at N.P.L., with a 13 ft × 9 ft octagonal working section. The maximum speed is about 240 ft/sec, but during the laminar-flow stability tests for which the tunnel has been frequently employed it has been found necessary to keep below 180 ft/sec in order to avoid premature transition. A honeycomb is fitted but there are no screens: the contraction ratio is only 4:1. The tunnel's unusual features are twin two-bladed fans in parallel circular ducts, and a freely rotating four-bladed windmill mounted in an *octagonal* section: the windmill supports have given trouble on several occasions and the windmill itself has recently had to be re-balanced.

The longitudinal component of turbulence rises from 0·04% at 10 ft/sec to 0·16% at 240 ft/sec (Fig. 10). There are pronounced peaks in the curve at 72, 120, 144, 180 and 208 ft/sec, the last three of which were found to be caused by windmill vibration as shown by the output from a resistance strain gauge bonded to one of the support struts. It is of course probable that the 72 ft/sec and 120 ft/sec peaks were also caused by the windmill, but the strain-gauge output at the lower speeds was difficult to measure. A frequency spectrum at 141 ft/sec is shown in Fig. 12.

Frequency spectra showed that the windmill contribution at twice and four times the shaft frequency is appreciable even at airspeeds away from the peaks in the intensity graph. The fan contribution is also noticeable but in this case no resonances were detected. The two motors are remotely controlled through a single pilot motor, with manual adjustment for synchronization which has only to be made occasionally. No tendency to beating was noticed and small departures from synchronism deliberately introduced had no effect on the turbulence: the effect on mean speed variations in the working section was not measured.

The lateral- and vertical-component intensities (w, v) rise steadily from 0·06% at 10 ft/sec to 0·23% at 210 ft/sec (Fig. 11), without any marked increase at the critical speeds mentioned above. A frequency spectrum at one of these critical speeds showed a fairly small windmill contribution (Fig. 13).

It is clear that the 'turbulence' in this tunnel is chiefly an inviscid mode of longitudinal pulsation caused by the windmill and, to a lesser extent, the fans. The windmill contribution is undoubtedly increased by the peculiar siting of the windmill in an octagonal section so that at the sides of the tunnel the blade tips are well clear of the walls whereas troughs are needed in roof and floor to prevent fouling: the airspeed over the tips of the blades therefore fluctuates severely during a revolution. If the windmill were removed, the turbulence level would be expected to decrease appreciably and might permit laminar-flow tests up to the maximum speed of the tunnel, but some attention would have to be given to the corner vanes in order to produce an acceptable mean velocity distribution. The components normal to the airstream are probably caused largely by working-section vibration.

3. *9 ft × 7 ft Tunnel (South)*[2] (*Fig.* 3).

There are two 9 ft × 7 ft Tunnels in the same building, identical except that one has right-hand corners and the other left-hand. The maximum speed is 230 ft/sec. The contraction ratio is 4:1, the same as that of the 13 ft × 9 ft Tunnel, but the 9 ft × 7 ft Tunnels have practically no settling length after the honeycomb. The longitudinal-component intensity rises only slightly with speed from about 0·17% at 60 ft/sec to 0·2% at 200 ft/sec (Fig. 14), and no resonant peaks were detected even though this tunnel, like the 13 ft × 9 ft, has audible resonances at several speeds. Clearly the chief sources of the velocity fluctuation are unsteadiness in the return circuit (the corner vanes are known to be inefficient) and turbulence shed from the honeycomb. In the 13 ft × 9 ft Tunnel, the long settling chamber reduces the latter, and the higher power factor (0·32 as against 0·22 for the 9 ft × 7 ft Tunnel, due to the absence of a diffuser before the first corner) may help to reduce the former.

The lateral-component intensity also rises slightly with speed, from about 0·18% at 70 ft/sec to 0·22% at 200 ft/sec (Fig. 15). The spectra (Figs. 16, 17) are unremarkable: the longitudinal component has a large low-frequency contribution absent from the lateral component, so that the return-circuit unsteadiness, which doubtless originates as a fluctuation in flow direction caused

by separations from corner vanes and diffuser walls, is reduced by the honeycomb to a longitudinal pulsation without any large fluctuations in flow direction. A similar but less pronounced effect is noted in the C.A.T.

4. 18 *in. Anemometer Tunnel*[3].

This tunnel has an open circuit, with a contraction ratio of 3·2 to 1. A honeycomb is fitted in the settling chamber. The fan has two blades. The maximum speed is 85 ft/sec: as the tunnel is frequently used for anemometer calibration down to very low airspeeds, perforated diaphragms can be fitted at the rear of the working section to improve speed control by using a low-blade-angle fan and keeping its thrust and speed high; sensitivity to draughts in the room is also reduced.

The longitudinal-component intensity in the unrestricted tunnel (Fig. 18) has a peak of about 0·28% at 25 ft/sec and thereafter remains approximately constant with speed at about 0·2%: slight peaks are noticeable at about 45 ft/sec and 67 ft/sec, caused by resonances at the fan-blade frequency as seen from the measured spectra (Fig. 21).

The lateral- and vertical-component intensities (Fig. 20) decreased with increasing speed from 0·35% at 20 ft/sec to 0·27% at 75 ft/sec. The spectrum (Fig. 22) indicates one predominant source of turbulence, clearly the honeycomb.

The longitudinal-component intensity with diaphragm 2 fitted is about 0·1% at the lowest speeds, less than that of the empty tunnel at the same fan speed, but rises to 0·25% at the maximum speed, which is now 13·5 ft/sec. The spectrum at this speed shows a very large contribution at the fan-blade frequency, with noticeable components at twice and four times that frequency.

The longitudinal component of turbulence with diaphragm 3 fitted rises from 0·2% at low speed, with occasional peaks, to 0·5% at the maximum speed of 3·8 ft/sec. The fan-blade frequency and its harmonics again make the largest contribution to the spectrum.

With diaphragm 4 fitted, the longitudinal component (Fig. 19) rises from about 0·4% to 1·3% at the maximum speed of 1·27 ft/sec: the speed ranges of the various diaphragms overlap so that the regions of very high turbulence need not be used for normal running. The fan *shaft* frequency now appears in the spectrum, indicating purely mechanical vibration due to unbalance of the fan or motor.

Spectrum peaks were also observed at certain fixed frequencies with all the diaphragms. The most important of these are at 33, 50, 60, 75 and 130 c/s approximately, and probably correspond to structural vibration frequencies or alternatively organ-pipe acoustic oscillations. The distance from the diaphragm position to the fan is 9·2 ft and that to the bellmouth 11 ft, corresponding to half-wavelengths of 61 and 50 c/s standing waves.

Conclusions.

Tunnel	$\frac{\tilde{u}}{\overline{U}}$ %	$\frac{\tilde{v}}{\overline{U}}$ %	Special Causes
	→ : increasing speed		
C.A.T.	0·3 → 0·6	0·3 → 0·7	vibration at high pressures
13 ft × 9 ft	0·05 → 0·18	0·06 → 0·23	windmill ($\tilde{u}$ component only)
9 ft × 7 ft	0·18	0·20	—
18 in. Anemometer	1·0 → 0·2	0·3	fan vibration when diaphragms installed for low-speed running

(86834)

Tunnel	Hot-wire System	Spectrum Analyser
C.A.T.	const. temperature	B + K passive filters
13 ft × 9 ft	const. current	Muirhead Wien bridge
9 ft × 7 ft	const. current	B + K passive filters
18 in. Anemometer	const. current	Muirhead Wien bridge

In all these tunnels, particularly the C.A.T. and 9 ft × 7 ft Tunnels, the turbulence is high by modern standards because of the absence of damping screens, compensated in the case of the 13 ft × 9 ft Tunnel by an unusually long settling chamber.

Installation of screens would be very difficult in the C.A.T. but less so in the 9 ft × 7 ft or 13 ft × 9 ft Tunnels: the 18 in. Tunnel was designed to accommodate screens if required.

The analysis of the turbulence in the 13 ft × 9 ft and 18 in. Tunnels also illustrates the importance of the fan and/or windmill as a source of disturbances. This is a difficulty common to all fan-powered wind tunnels, even when a low random-turbulence level is not specially required, as unpleasant noise or even structural fatigue may result: unfortunately considerations of space and expense often prohibit the use of a sufficiently low fan speed to avoid vibration.

REFERENCES

No.	*Author(s)*	*Title, etc.*
1	P. Bradshaw and R. F. Johnson ..	Turbulence measurements with hot wire anemometers. N.P.L. Note on Applied Science, No. 33. H.M.S.O. 1963.
2	E. J. Richards and F. Cheers ..	Notes on the N.P.L. 13 ft × 9 ft and 9 ft × 7 ft Wind Tunnels. A.R.C. R. & M. 2136. July, 1945.
3	C. Salter	Low speed wind tunnels for special purposes. NPL/Aero/155. 1947.

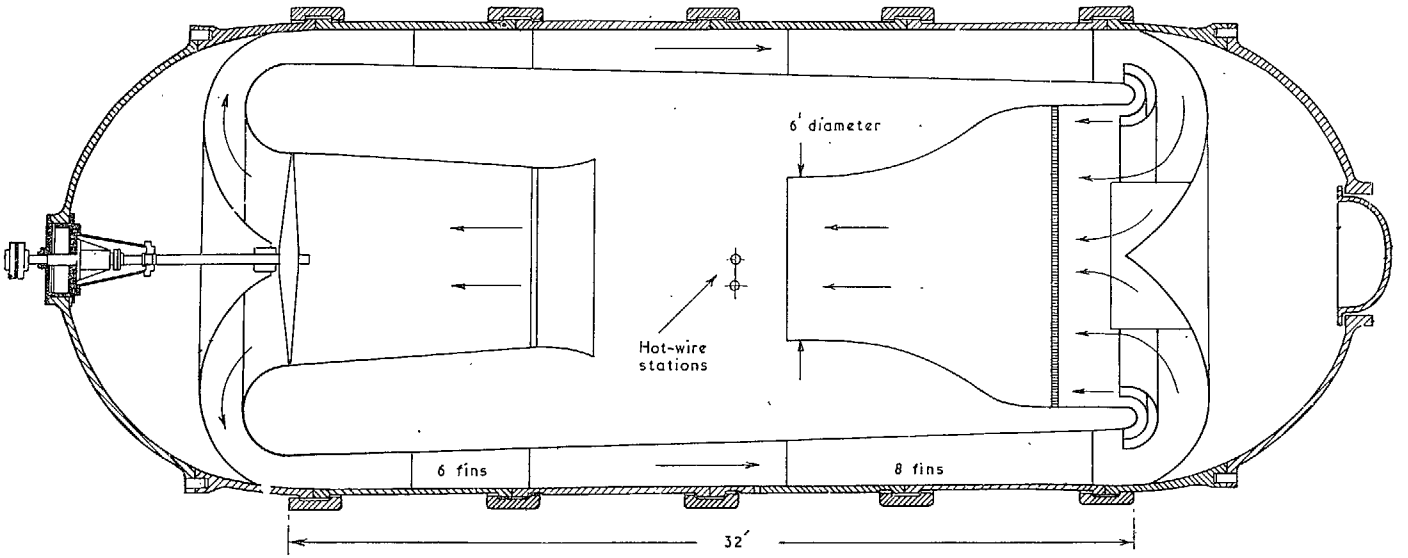

FIG. 1. Plan view of Compressed Air Tunnel.

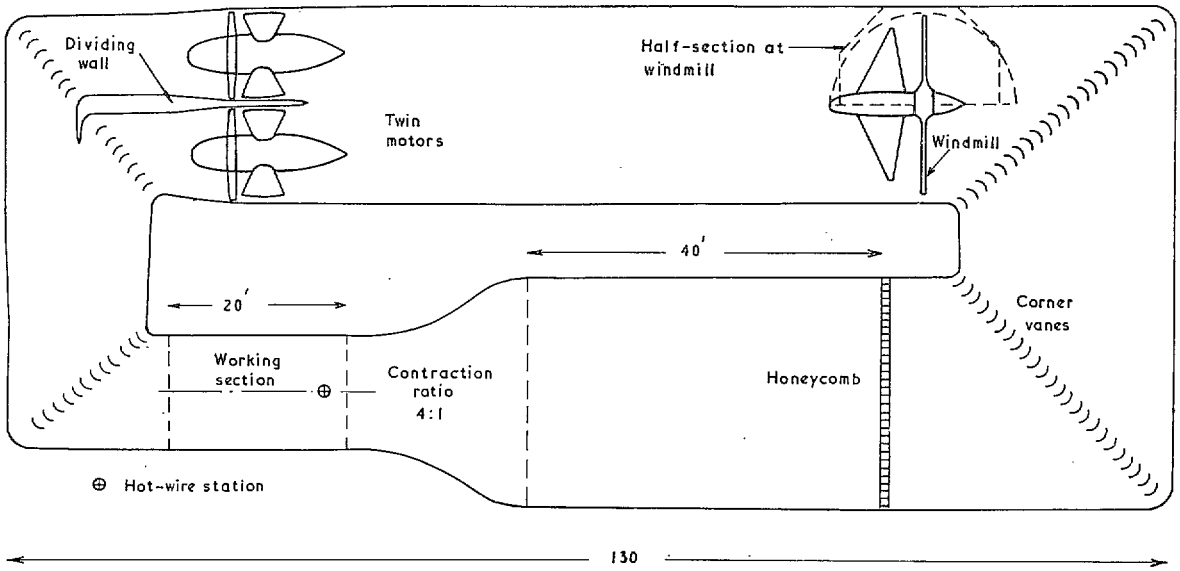

FIG. 2. 13 ft × 9 ft Wind Tunnel.

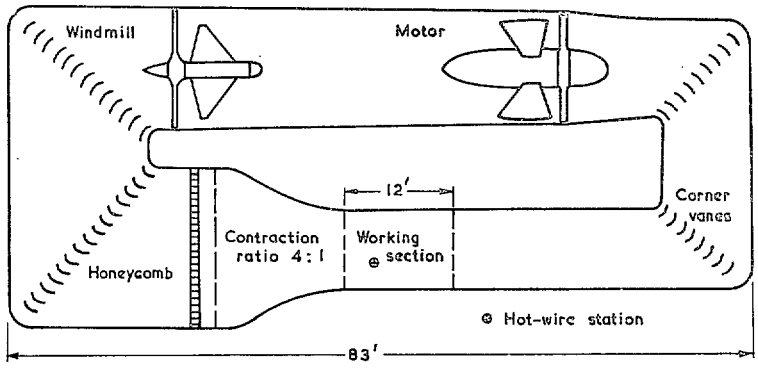

FIG. 3. 9 ft × 7 ft Wind Tunnel.

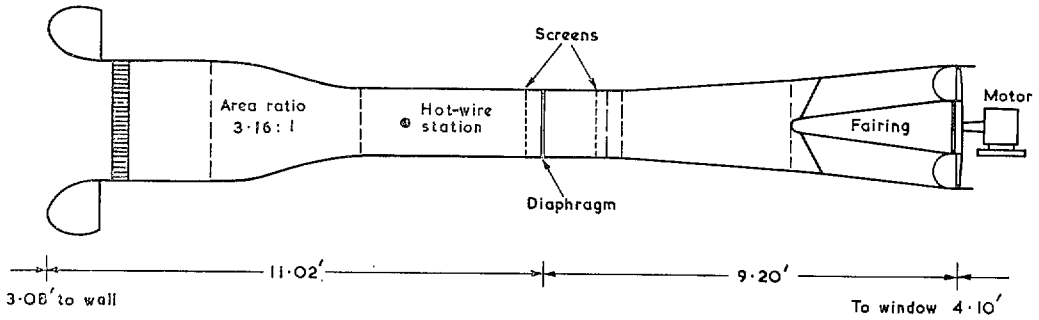

FIG. 4. 18 in. Anemometer Tunnel.

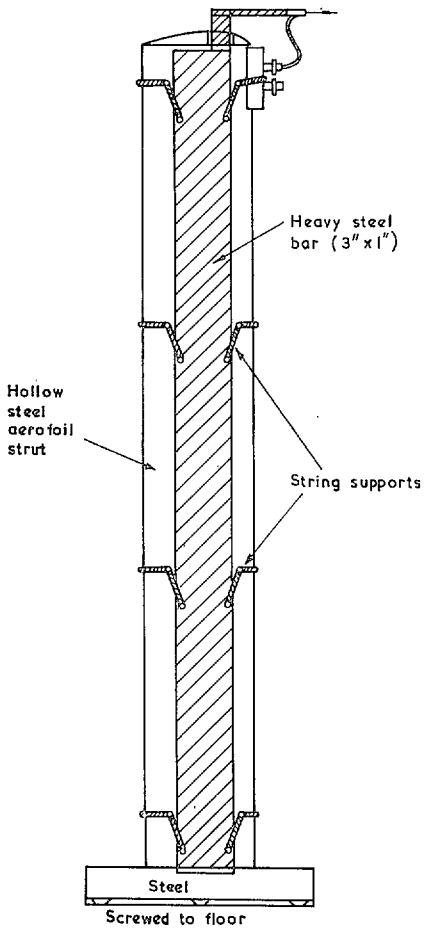

FIG. 5. Hot-wire mounting strut.

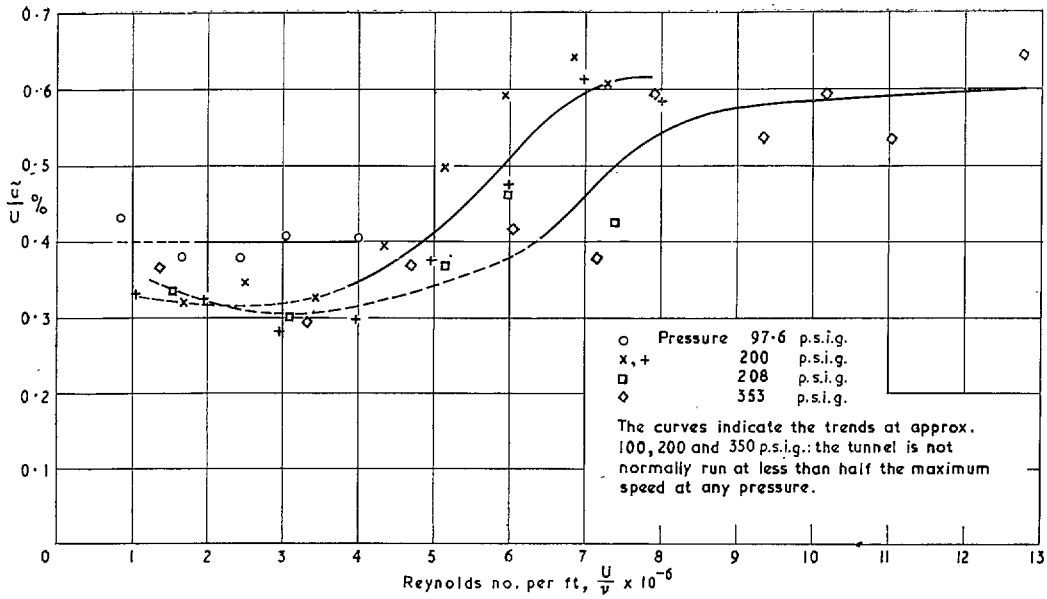

FIG. 6a. *u*-component r.m.s. intensity in C.A.T.

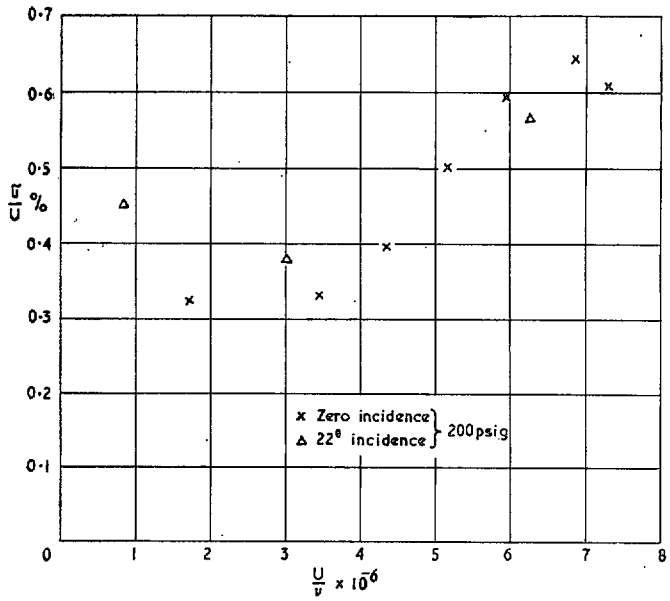

FIG. 6b. *u*-component r.m.s. intensity in C.A.T.: effect of changing model-wing incidence. 49° swept wing, area $3\frac{1}{4}$ ft², aspect ratio 3.

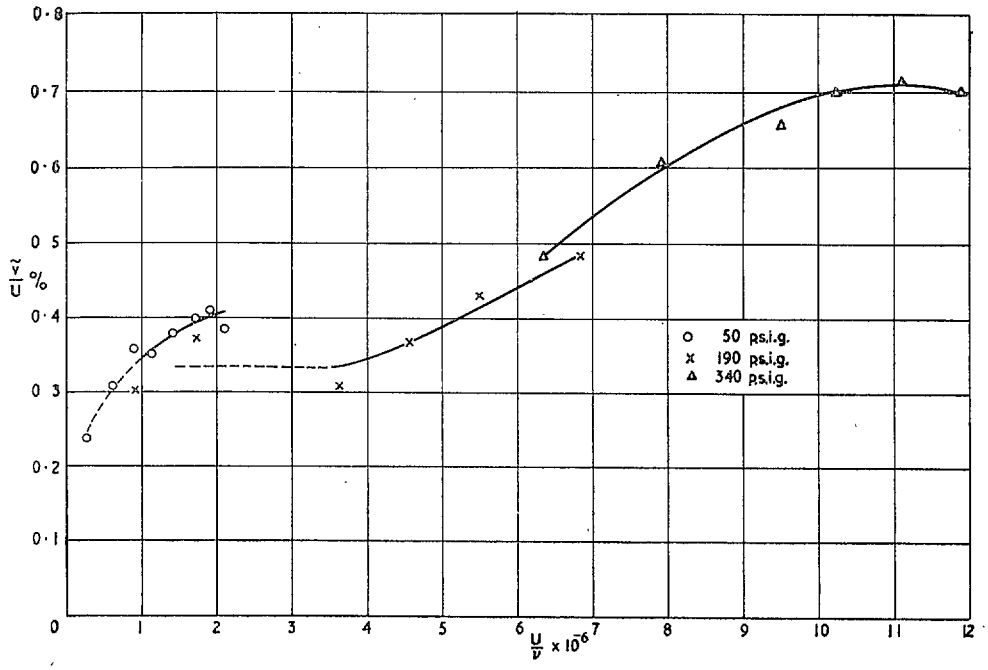

FIG. 7. v-component r.m.s. intensity in C.A.T.

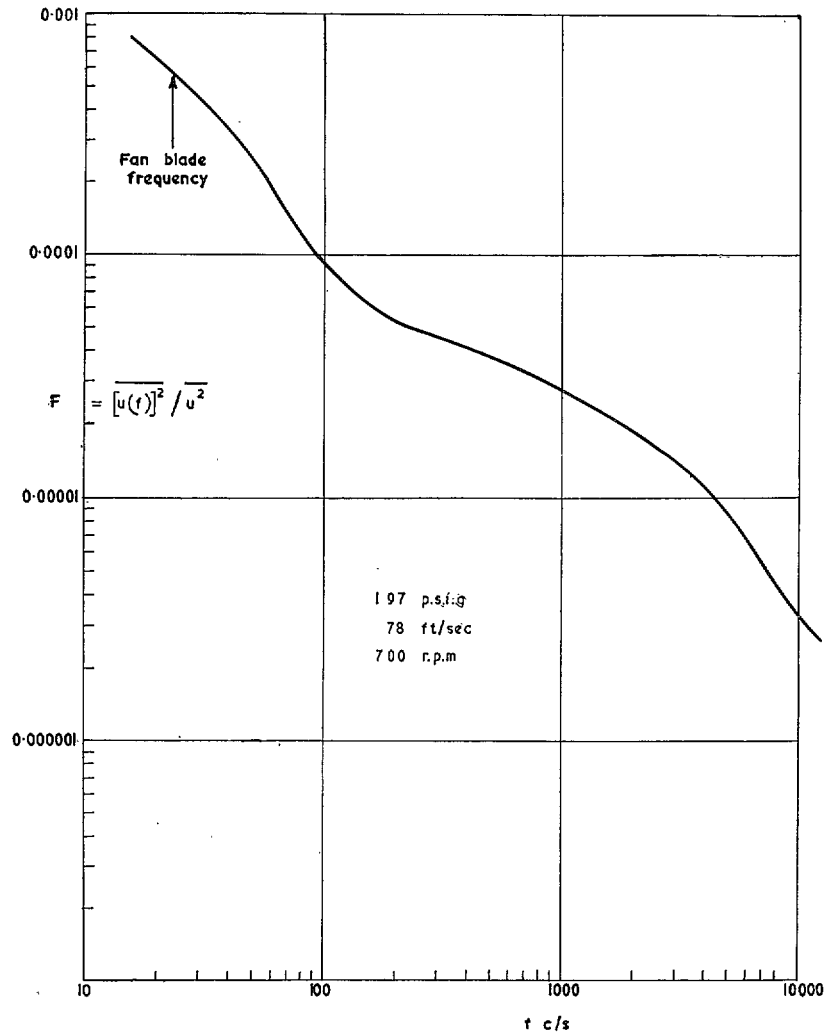

FIG. 8. *u*-component spectrum in C.A.T.

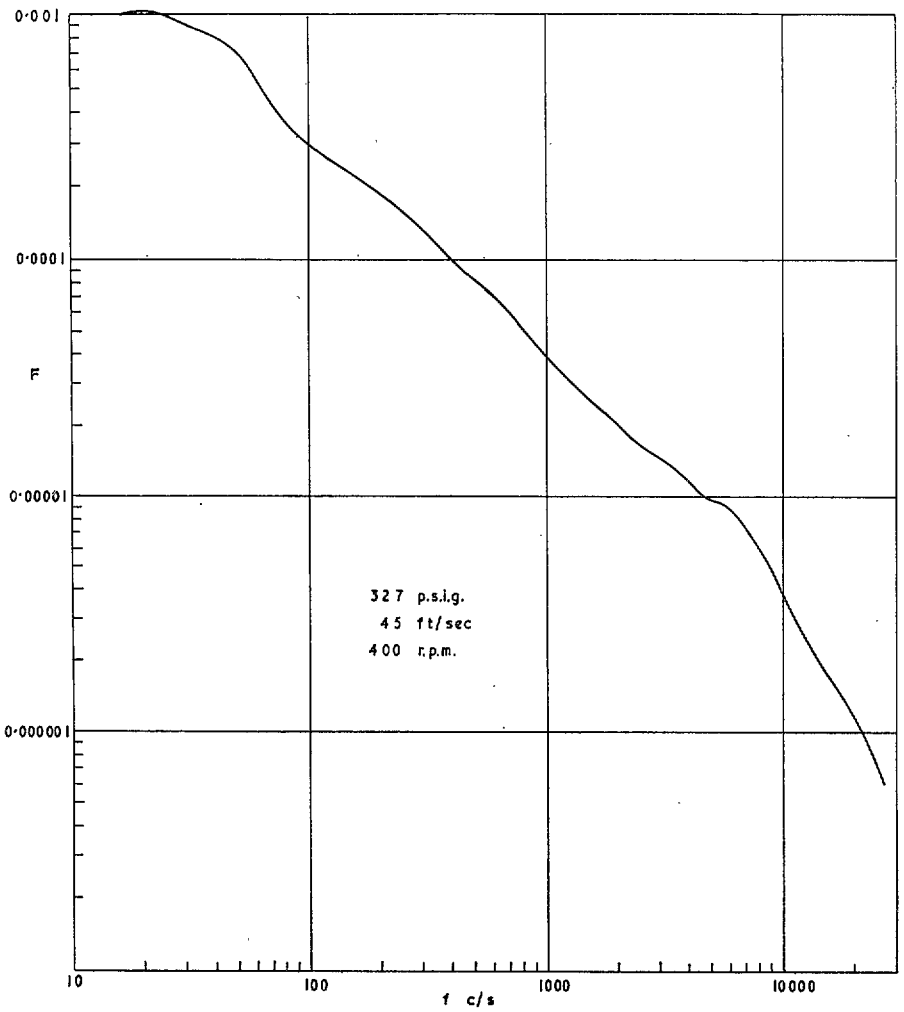

FIG. 9. v-component spectrum in C.A.T.

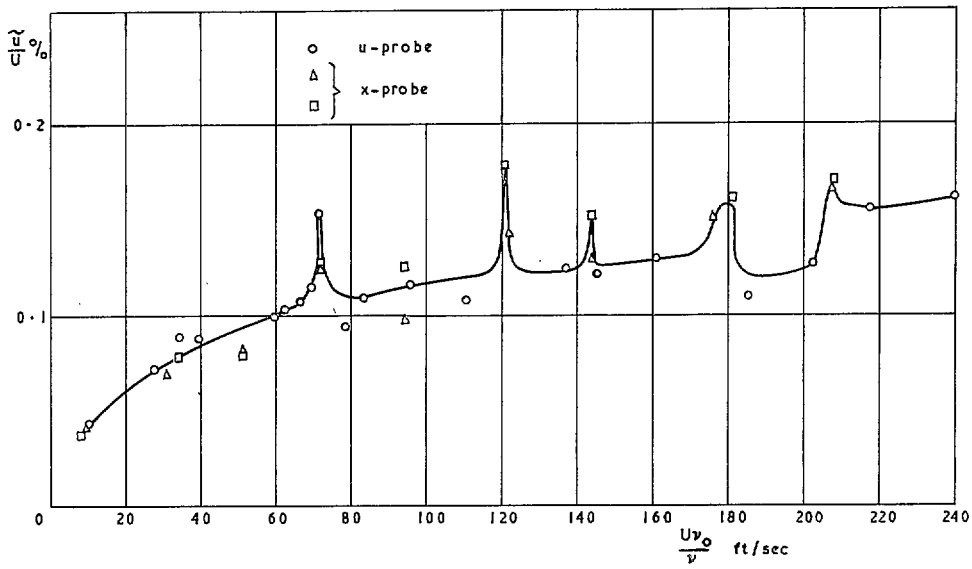

FIG. 10. *u*-component r.m.s. intensity in 13 ft × 9 ft Tunnel.

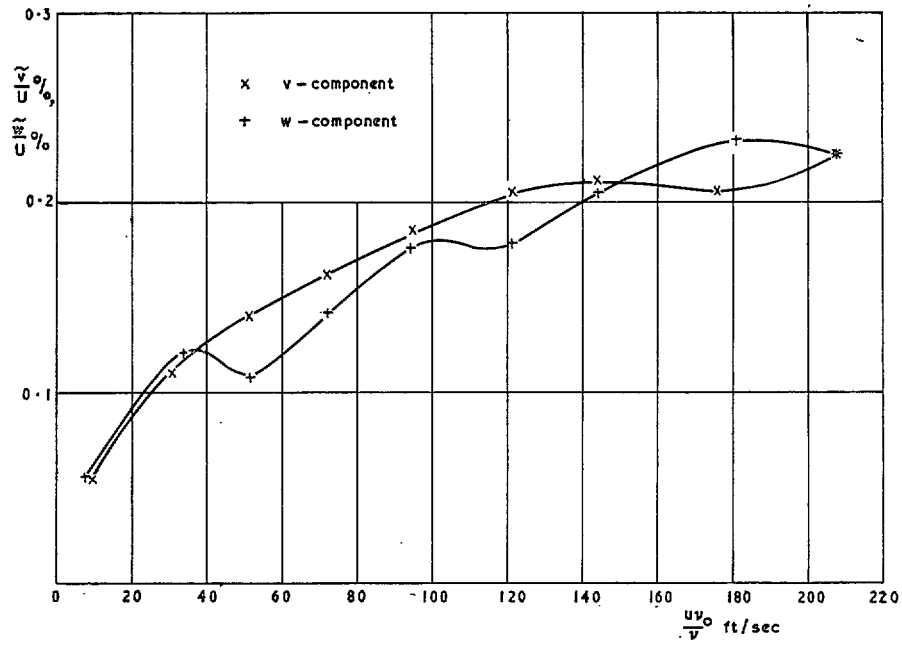

FIG. 11. *v*- and *w*-component r.m.s. intensities in 13 ft × 9 ft Tunnel.

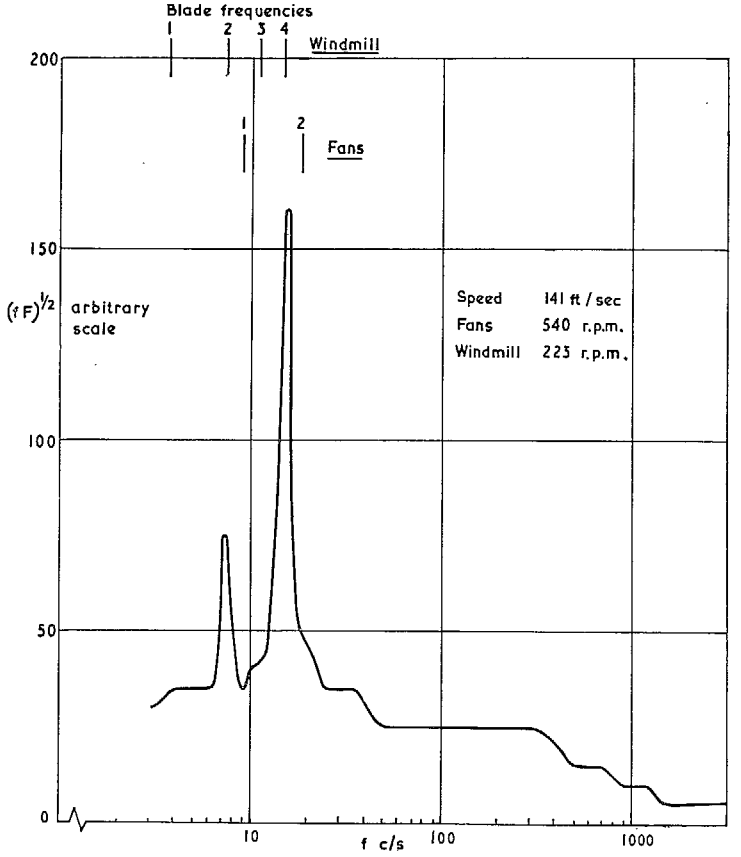

FIG. 12. *u*-component spectrum in 13 ft × 9 ft Tunnel.

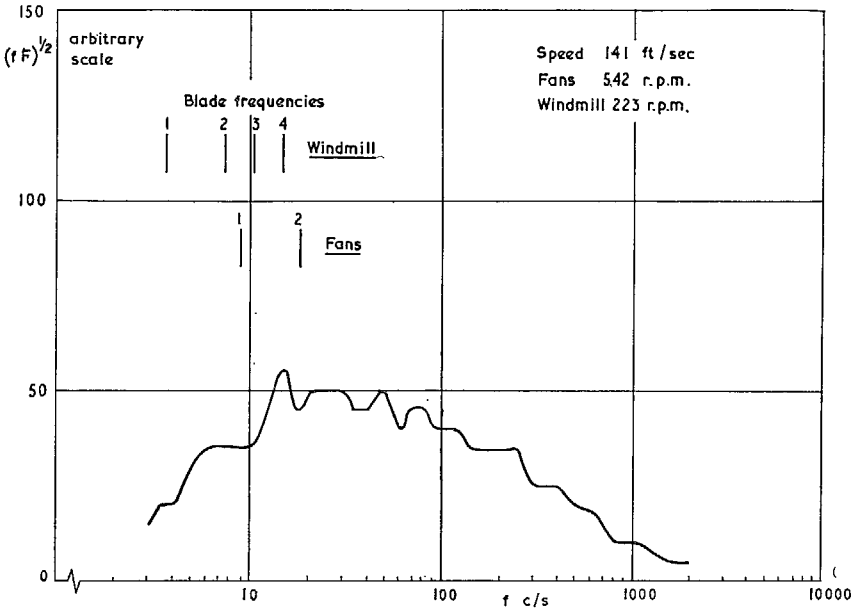

FIG. 13. *v*-component spectrum in 13 ft × 9 ft Tunnel.

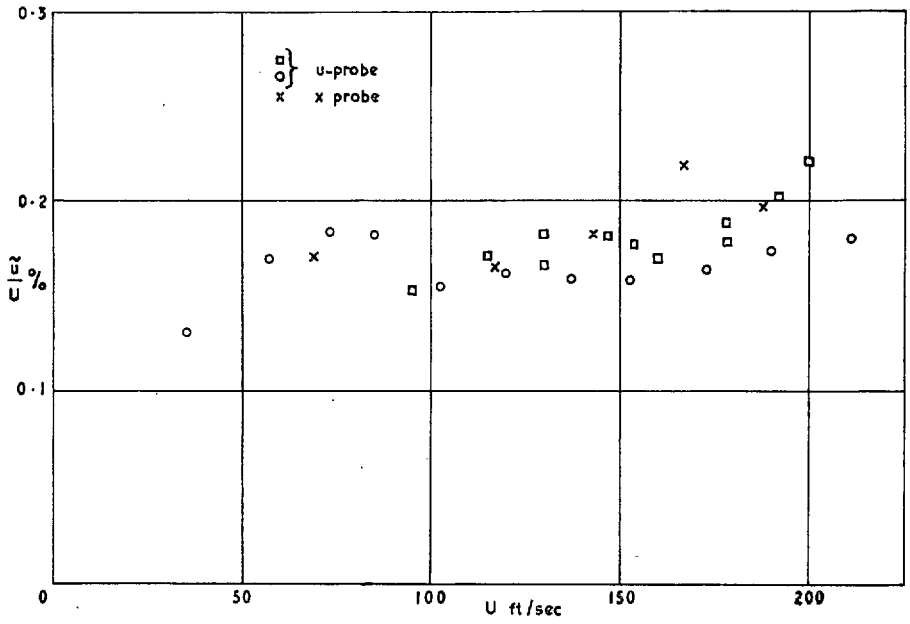

FIG. 14. *u*-component r.m.s. intensity in 9 ft × 7 ft Tunnel.

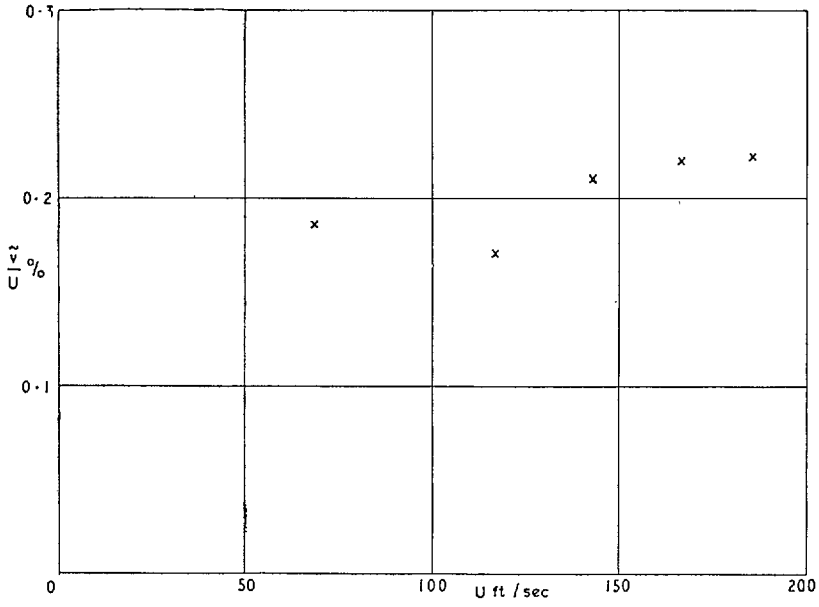

FIG. 15. *v*-component r.m.s. intensity in 9 ft × 7 ft Tunnel.

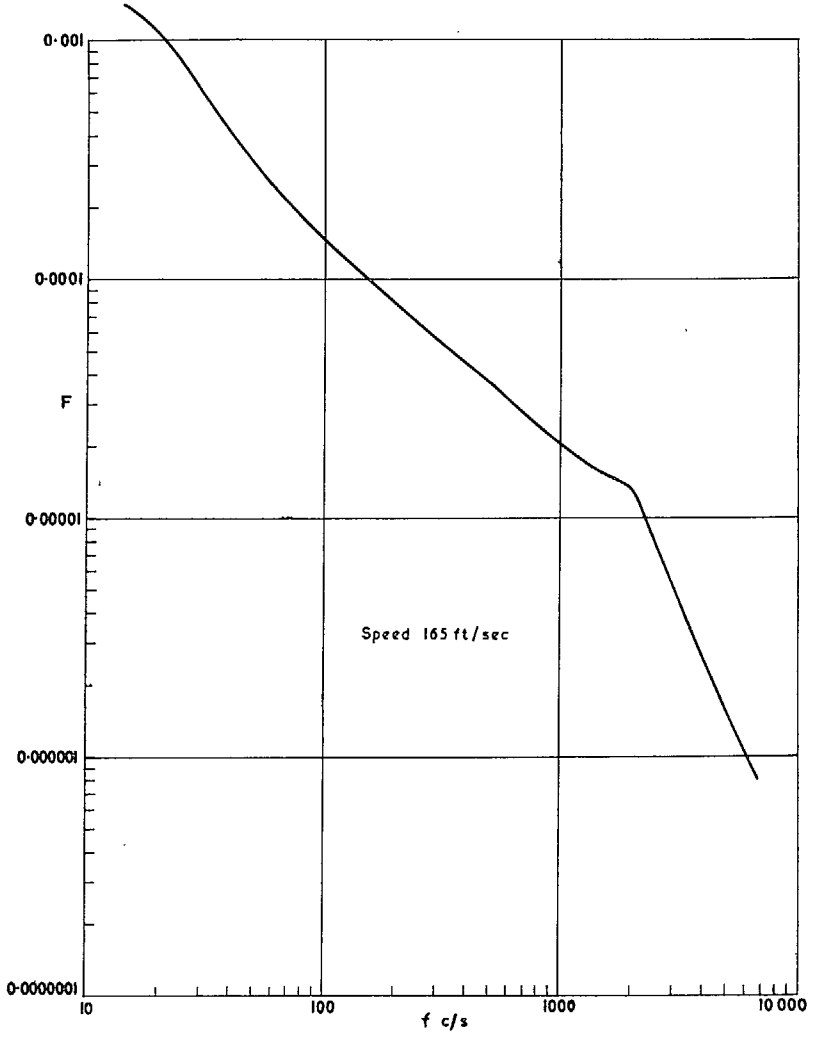

FIG. 16. *u*-component spectrum in 9 ft × 7 ft Tunnel.

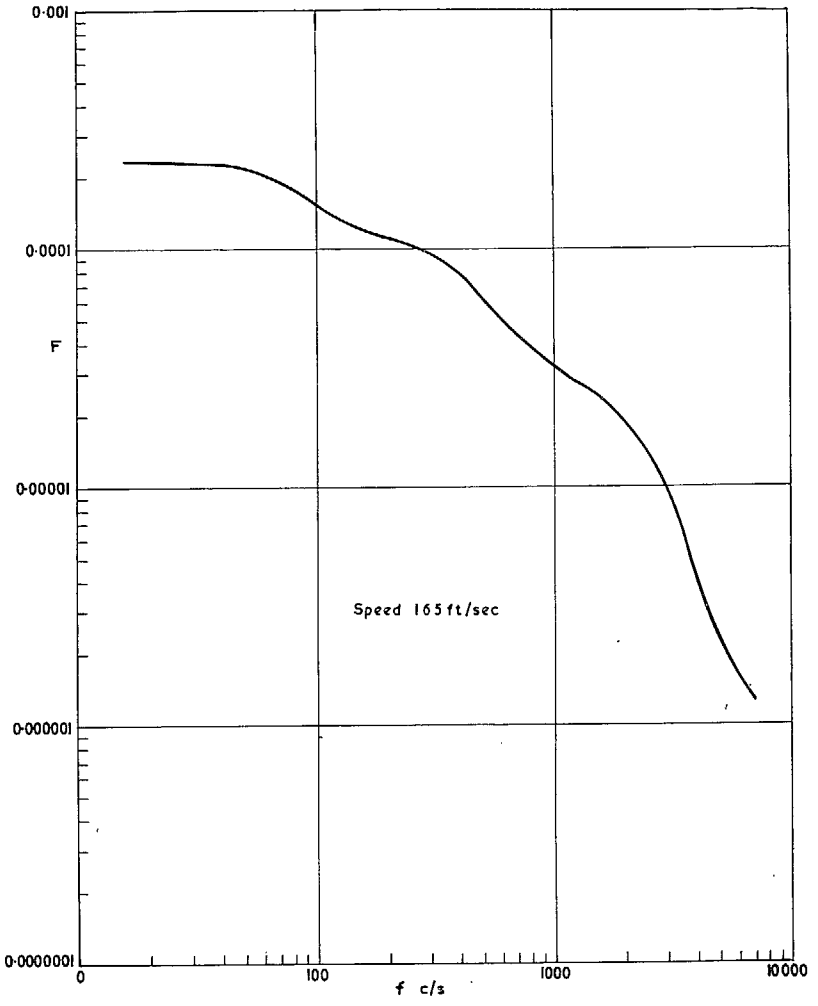

FIG. 17. *v*-component spectrum in 9 ft × 7 ft Tunnel.

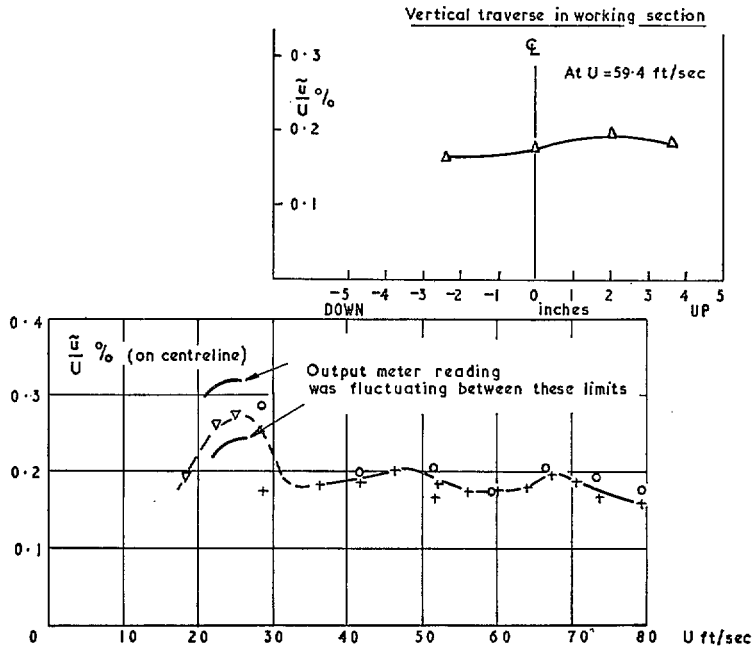

FIG. 18. *u*-component r.m.s. intensity in Anemometer Tunnel. Unrestricted tunnel.

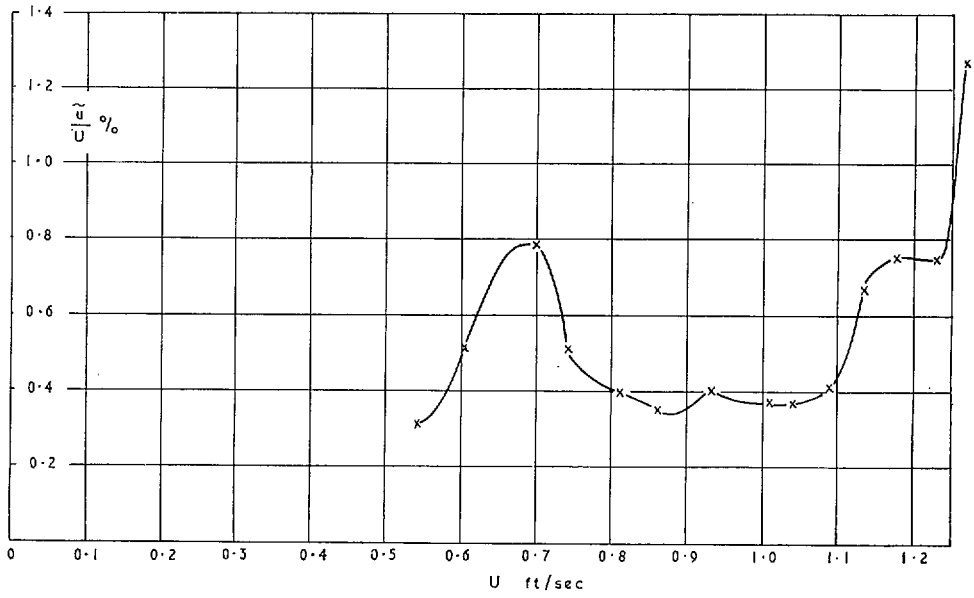

FIG. 19. *u*-component r.m.s. intensity in Anemometer Tunnel. Diaphragm No. 4.

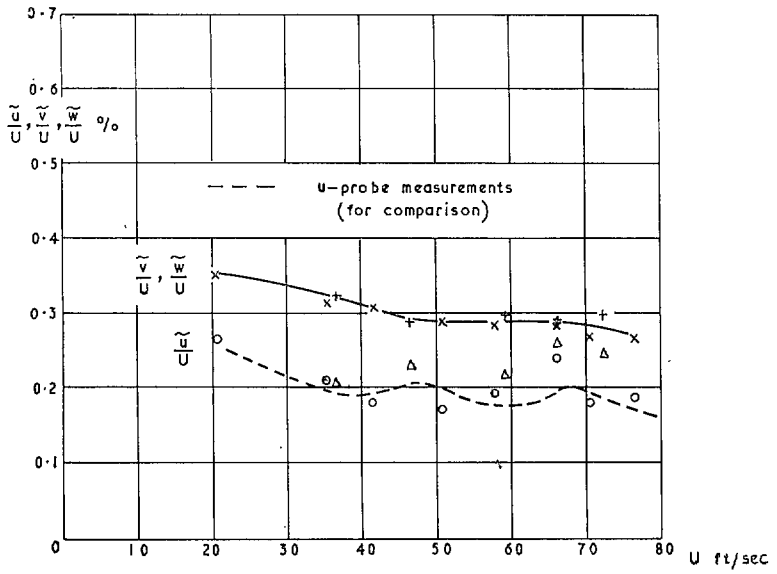

FIG. 20. *v*- and *w*-component r.m.s. intensities in Anemometer Tunnel, and *u*-component measurements with x-probe. Unrestricted tunnel.

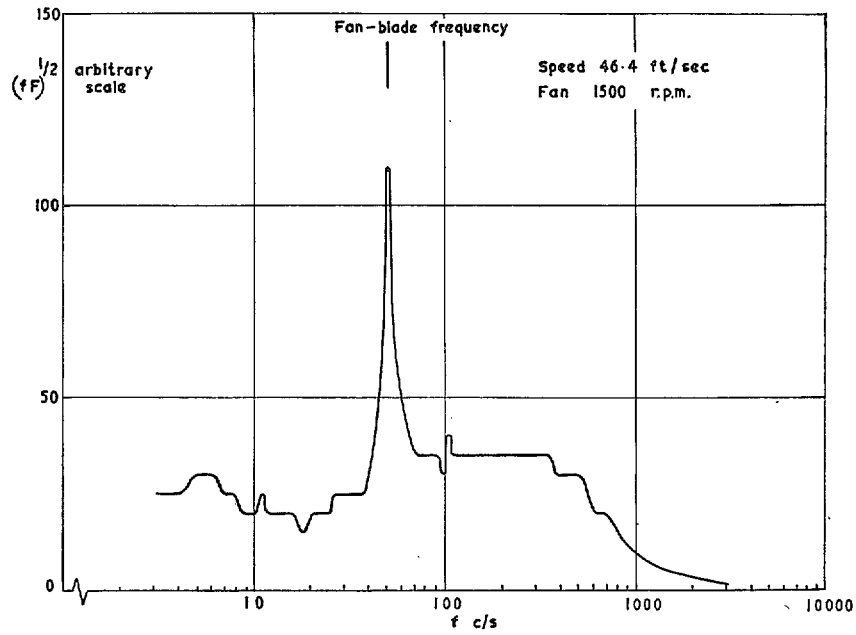

FIG. 21. *u*-component spectrum in Anemometer Tunnel. Unrestricted tunnel.

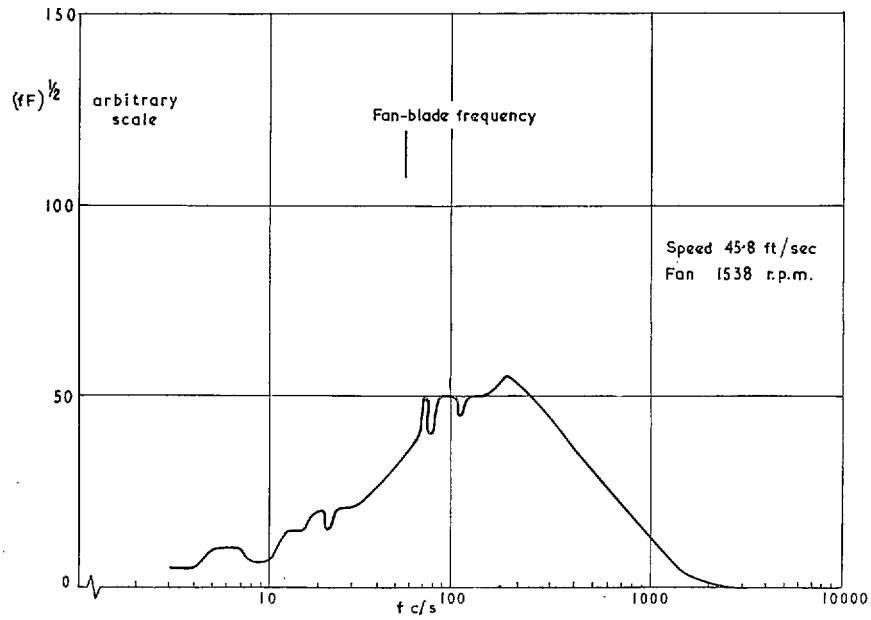

FIG. 22. *v*-component spectrum in Anemometer Tunnel. Unrestricted tunnel.

(86834) Wt. 64/1857 K5 4/63 Hw.

Publications of the Aeronautical Research Council

ANNUAL TECHNICAL REPORTS OF THE AERONAUTICAL RESEARCH COUNCIL (BOUND VOLUMES)

1942 Vol. I. Aero and Hydrodynamics, Aerofoils, Airscrews, Engines. 75*s.* (post 2*s.* 9*d.*)
Vol. II. Noise, Parachutes, Stability and Control, Structures, Vibration, Wind Tunnels. 47*s.* 6*d.* (post 2*s.* 3*d.*)

1943 Vol. I. Aerodynamics, Aerofoils, Airscrews. 80*s.* (post 2*s.* 6*d.*)
Vol. II. Engines, Flutter, Materials, Parachutes, Performance, Stability and Control, Structures. 90*s.* (post 2*s.* 9*d.*)

1944 Vol. I. Aero and Hydrodynamics, Aerofoils, Aircraft, Airscrews, Controls. 84*s.* (post 3*s.*)
Vol. II. Flutter and Vibration, Materials, Miscellaneous, Navigation, Parachutes, Performance, Plates and Panels, Stability, Structures, Test Equipment, Wind Tunnels. 84*s.* (post 3*s.*)

1945 Vol. I. Aero and Hydrodynamics, Aerofoils. 130*s.* (post 3*s.* 6*d.*)
Vol. II. Aircraft, Airscrews, Controls. 130*s.* (post 3*s.* 6*d.*)
Vol. III. Flutter and Vibration, Instruments, Miscellaneous, Parachutes, Plates and Panels, Propulsion. 130*s.* (post 3*s.* 3*d.*)
Vol. IV. Stability, Structures, Wind Tunnels, Wind Tunnel Technique. 130*s.* (post 3*s.* 3*d.*)

1946 Vol. I. Accidents, Aerodynamics, Aerofoils and Hydrofoils. 168*s.* (post 3*s.* 9*d.*)
Vol. II. Airscrews, Cabin Cooling, Chemical Hazards, Controls, Flames, Flutter, Helicopters, Instruments and Instrumentation, Interference, Jets, Miscellaneous, Parachutes. 168*s.* (post 3*s.* 3*d.*)
Vol. III. Performance, Propulsion, Seaplanes, Stability, Structures, Wind Tunnels. 168*s.* (post 3*s.* 6*d.*)

1947 Vol. I. Aerodynamics, Aerofoils, Aircraft. 168*s.* (post 3*s.* 9*d.*)
Vol. II. Airscrews and Rotors, Controls, Flutter, Materials, Miscellaneous, Parachutes, Propulsion, Seaplanes, Stability, Structures, Take-off and Landing. 168*s.* (post 3*s.* 9*d.*)

1948 Vol. I. Aerodynamics, Aerofoils, Aircraft, Airscrews, Controls, Flutter and Vibration, Helicopters, Instruments, Propulsion, Seaplane, Stability, Structures, Wind Tunnels. 130*s.* (post 3*s.* 3*d.*)
Vol. II. Aerodynamics, Aerofoils, Aircraft, Airscrews, Controls, Flutter and Vibration, Helicopters, Instruments, Propulsion, Seaplane, Stability, Structures, Wind Tunnels. 110*s.* (post 3*s.* 3*d.*)

Special Volumes

Vol. I. Aero and Hydrodynamics, Aerofoils, Controls, Flutter, Kites, Parachutes, Performance, Propulsion, Stability. 126*s.* (post 3*s.*)
Vol. II. Aero and Hydrodynamics, Aerofoils, Airscrews, Controls, Flutter, Materials, Miscellaneous, Parachutes, Propulsion, Stability, Structures. 147*s.* (post 3*s.*)
Vol. III. Aero and Hydrodynamics, Aerofoils, Airscrews, Controls, Flutter, Kites, Miscellaneous, Parachutes, Propulsion, Seaplanes, Stability, Structures, Test Equipment. 189*s.* (post 3*s.* 9*d.*)

Reviews of the Aeronautical Research Council

1939–48 3*s.* (post 6*d.*) 1949–54 5*s.* (post 5*d.*)

Index to all Reports and Memoranda published in the Annual Technical Reports

1909–1947 R. & M. 2600 (out of print)

Indexes to the Reports and Memoranda of the Aeronautical Research Council

Between Nos. 2351–2449	R. & M. No. 2450	2*s.* (post 3*d.*)
Between Nos. 2451–2549	R. & M. No. 2550	2*s.* 6*d.* (post 3*d.*)
Between Nos. 2551–2649	R. & M. No. 2650	2*s.* 6*d.* (post 3*d.*)
Between Nos. 2651–2749	R. & M. No. 2750	2*s.* 6*d.* (post 3*d.*)
Between Nos. 2751–2849	R. & M. No. 2850	2*s.* 6*d.* (post 3*d.*)
Between Nos. 2851–2949	R. & M. No. 2950	3*s.* (post 3*d.*)
Between Nos. 2951–3049	R. & M. No. 3050	3*s.* 6*d.* (post 3*d.*)
Between Nos. 3051–3149	R. & M. No. 3150	3*s.* 6*d.* (post 3*d.*)

HER MAJESTY'S STATIONERY OFFICE

from the addresses overleaf

Printed and published by
HER MAJESTY'S STATIONERY OFFICE

To be purchased from
York House, Kingsway, London W.C.2
423 Oxford Street, London W.1
13A Castle Street, Edinburgh 2
109 St. Mary Street, Cardiff
39 King Street, Manchester 2
50 Fairfax Street, Bristol 1
35 Smallbrook, Ringway, Birmingham 5
80 Chichester Street, Belfast 1
or through any bookseller

Printed in England

S.O. Code No. 23-3317